THE JOURNAL OF BIOLOGICAL CHEMISTRY VOL. 286, NO. 35, pp. 30780–30794, September 2, 2011

Cell Entry of Avian Reovirus Follows a Caveolin-1-mediated and Dynamin-2-dependent Endocytic Pathway That Requires Activation of p38 Mitogen-activated Protein Kinase (MAPK) and Src Signaling Pathways as Well as Microtubules and Small GTPase Rab5 Protein*[S]

Received for publication, May 25, 2011, and in revised form, June 24, 2011 Published, JBC Papers in Press, June 26, 2011, DOI 10.1074/jbc.M111.257154

Wei R. Huang[‡], Ying C. Wang[‡§], Pei I. Chi[‡§], Lai Wang[‡], Chi Y. Wang[¶], Chi H. Lin[‖], and Hung J. Liu[‡1]

From the [‡]Institute of Molecular Biology, National Chung Ching University, Taichung 402, the [§]Graduate Institute of Biotechnology, National Pingtung University of Science and Technology, Pingtung 912, the [¶]Department of Veterinary Medicine, National Chung Ching University, Taichung 402, and the [‖]Institute of Microbiology and Immunology, National Yang-Ming University, Taipei 11221, Taiwan

Very little is known about the mechanism of cell entry of avian reovirus (ARV). The aim of this study was to explore the mechanism of ARV entry and subsequent infection. Cholesterol mainly affected the early steps of the ARV life cycle, because the presence of cholesterol before and during viral adsorption greatly blocked ARV infectivity. Although we have demonstrated that ARV facilitating p38 MAPK is beneficial for virus replication, its mechanism remains unknown. Here, we show that ARV-induced phosphorylation of caveolin-1 (Tyr^{14}), dynamin-2 expression, and Rac1 activation through activation of p38 MAPK and Src in the early stage of the virus life cycle is beneficial for virus entry and productive infection. The strong inhibition by dynasore, a specific inhibitor of dynamin-2, and depletion of endogenous caveolin-1 or dynamin-2 by siRNAs as well as the caveolin-1 colocalization study implicate caveolin-1-mediated and dynamin-2-dependent endocytosis as a significant avenue of ARV entry. By means of pharmacological inhibitors, dominant negative mutants, and siRNA of various cellular proteins and signaling molecules, phosphorylation of caveolin-1, dynamin-2 expression, and Rac1 activation were suppressed, suggesting that by orchestrating p38 MAPK, Src, and Rac1 signaling cascade in the target cells, ARV creates an appropriate intracellular environment facilitating virus entry and productive infection. Furthermore, disruption of microtubules, Rab5, or endosome acidification all inhibited ARV infection, suggesting that microtubules and small GTPase Rab5, which regulate transport to early endosome, are crucial for survival of ARV and that exposure of the virus to acidic pH is required for productive infection.

Viral infection is usually initiated by binding of viral attachment proteins with a specific receptor(s) on the cell membrane, which subsequently leads to internalization of the virus into cells. After virus attachment to its respective cell-surface receptor, internalization usually proceeds via either from the plasma membrane or endocytosis. Two well characterized endocytic pathways include clathrin-dependent and lipid raft and caveola-dependent endocytosis. In clathrin-mediated endocytosis, clathrin is first recruited to the plasma membrane in response to receptor-mediated internalization signals, which then results in the assembly of CCPs[2] at the cytoplasmic side of the cell membrane. Clathrin possessing light chain and heavy chain forms a unique structure called clathrin triskelion (1). During the assembly of CCPs, the AP-2 protein provides a connection between receptors' cargo domain and the clathrin coat, which occurs through binding of the $\mu 2$ subunit of AP-2 to both the receptors' cargo domain and the clathrin β subunit (2). Once assembled, CCPs pinch off from the cell membrane and mature into clathrin-coated vesicles (1), which then transfer the cargo into endosomes. To date, a number of viruses enter into host cells through the clathrin-dependent endocytosis pathway (3–5). The clathrin-independent pathways include a caveola-dependent pathway. Caveolae, small uncoated pits in the membrane, are relatively small vesicles 50–100 nm in diameter, formed by membrane invagination at the cell surface, and coated by caveolin-1 (6). Caveolin-1 and -2 are coexpressed in most cell types, whereas the expression of caveolin-3 is muscle-specific (7). Membrane rafts are small, mobile, and unstable, which fluctuate in composition and size (8). Cholesterol is integral to the formation and maintenance of caveolae, and depletion of cholesterol causes flattening of caveolae (9). They have been found to mediate many biological events such as signal transduction pathway, endocytic traffic, synthetic traffic, and virus replication cycle (9, 10). Dynamin is a GTPase required for the cellular membrane to pinch off endosomes from the plasma membrane and is necessary for clathrin- and caveola-mediated endocytosis and phagocytosis, but it is not required for macropinocytosis (11, 12). Caveolae have been shown to provide a

* This work was supported by National Science Council of Taiwan Grants NSC99-2321-B-005-015-MY3 and NSC97-2313-B-005-048-MY3.

[S] The on-line version of this article (available at http://www.jbc.org) contains supplemental Figs. 1 and 2.

[1] To whom correspondence should be addressed. Tel.: 886-4-22840485 (Ext. 243); Fax: 886-4-22874879; E-mail: hjliu5257@nchu.edu.tw.

[2] The abbreviations used are: CCP, clathrin-coated pit; ARV, avian reovirus; MβCD, methyl-β-cyclodextrin; BEFV, bovine ephemeral fever virus; DN, dominant negative; CPZ, chlorpromazine; m.o.i., multiplicity of infection; Csk, C-terminal Src kinase; GTPγS, guanosine 5′-3-*O*-(thio)triphosphate; MEM, minimum essential medium.

vehicle for the entry of many viruses into animal cells (13–16). For example, simian virus 40 (SV40) utilizes caveolae to be internalized under a neutral conditions (17). However, internalization of SV40 was also found in cells that do not express caveolin-1, suggesting that SV40 utilizes not only the caveola-dependent pathway but also the lipid raft-dependent and caveola-independent pathway (18).

Enveloped virus infection is initiated by the viral glycoprotein binding to its cellular receptor. The binding event either triggers membrane fusion at the plasma membrane or internalization of the virus into an endosome. For those viruses that are endocytosed, subsequent endosomal events lead to fusion of the viral membrane with the vesicle, releasing the core particle into the cytoplasm. A number of these pathways traffic through acidic compartments. Viruses can take advantage of the lower pH environment to promote events that trigger membrane fusion (19–21).

ARV belongs to the Reoviridae family, and ARV is an important pathogen in poultry. Sharing much similarity with mammalian reoviruses, the virion particles of ARV possess two layers of capsid and 10 genome segments of double-stranded RNA. The genome segments are grouped into three size classes, designated L (large), M (medium), and S (small), depending on their electrophoretic mobility, that encode at least eight structural and four nonstructural proteins. In the S class segments of ARV, segment S1 contains three open reading frames that are translated into p10, p17, and σC proteins. ARV differs from their mammalian counterparts by its ability to cause massive cell fusion through the protein p10 (22, 23). More recently, the nonstructural protein p17 is reported to regulate the cell cycle and host cellular translation (24). The avian reovirus fiber is formed by capsid protein σC and is encoded by the third open reading frame of the S1 segment, which is responsible for host cell attachment (25, 26) and induction of apoptosis (27).

For the past several years, our laboratory has been studying molecular evolution of ARV and signaling pathways triggered by ARV required for apoptosis induction, virus replication, and cell cycle perturbations (22, 27–33). To date, the molecular events leading to endocytosis by ARV are still completely unknown. In this study, we have undertaken a comprehensive investigation of ARV entry to determine how ARV proceeds from internalization to uncoating. Using specific inhibitors and hypertonic medium, together with siRNAs, DN mutants, and Csk, we demonstrate that ARV enters host cells through the caveolin-1-mediated and dynamin-2-dependent pathways and that ARV-induced activation of Ras, p38 MAPK, and Src facilitates virus entry and activation of Rac1 that is beneficial for virus replication. Furthermore, we have first uncovered that the small GTPase Rab5 and the microtubules regulating transport to early endosome are required for ARV infection.

EXPERIMENTAL PROCEDURES

Antibodies—A monoclonal antibody against ARV σC protein was from our laboratory stock (34). Rabbit anti-dynamin-2 polyclonal antibody was from Abcam Co. (Cambridge, MA). Rabbit anti-p-p38 MAPK (Thr^{180}/Tyr^{182}), rabbit anti-p38 MAPK, rabbit anti-p-Src (Tyr^{418}), rabbit anti-Src, rabbit anti-p-caveolin-1 (Tyr^{14}), and Rac1 antibodies were from Cell Signaling Technology (Danvers, MA). Mouse anti-caveolin-1 monoclonal antibody was purchased from BD Biosciences.

Chemical Inhibitors—The mechanism of ARV cell entry was investigated by using different inhibitors of endocytosis. CPZ, MβCD, nystatin, cholesterol, dynasore, sucrose, NH_4Cl, nocodazole, chloroquine, PP2 (Src inhibitor), and SB202190 (p38 MAPK inhibitor) were purchased from Sigma. NSC23766 (Rac1 inhibitor) and bafilomycin A1 were from Calbiochem. Cytochalasin D was purchased from MG Scientific Inc. (San Diego).

CPZ, known to prevent assembly of coated pits at the plasma membrane, was used to disrupt clathrin-mediated endocytosis (35). MβCD and nystatin were used to block cholesterol-dependent, raft/caveola-mediated endocytosis. Dynasore is a small molecule inhibitor of the dynamin GTPase activity that prevents the scission of clathrin-coated pits from the plasma membrane (36). Bafilomycin A1, a specific inhibitor of the vacuolar H^+-ATPase (37), was used to inhibit the vacuolar H^+-ATPase, and its use leads to alkalinization of acidic organelles, including endosomes and lysosomes. Cytochalasin D and nocodazole were used to disrupt actin filament and microtubules (38), respectively.

Cells and Viruses—Vero and DF-1 cells were maintained in minimum essential medium (MEM) supplemented with 10% FBS and 10 mM HEPES (pH 7.2). Cells were seeded in 6-cm cell culture dishes with 1×10^6 cells 1 day before each experiment in a 37 °C incubator with 5% CO_2. All experimental procedures were started after refreshing the MEM containing 2% FBS overnight once cell confluence reached about 75%. The S1133 strain of ARV was propagated in DF-1 cells. At about 70–80% cytopathic effect, the supernatant was harvested and stored at −70 °C for further studies.

Virus Titration—Supernatants from ARV-infected cells were collected after 24 h, and relative progeny virus titer of ARV was determined by plaque assays in all experiments in this study. Cells in 6-cm cell culture dishes were incubated with diluted virus in 100 μl of serum-free MEM. The cells were then washed twice with MEM to remove unabsorbed virus and overlaid with 0.5 ml of 1% agarose in MEM containing 2% FBS and antibiotics. Plaques were visualized after an incubation period of 2–3 days at 37 °C by staining overnight with neutral red.

Effect of Cholesterol Depletion on ARV Production—A pharmacological approach involves the treatment of cells with MβCD that depletes the membrane of cholesterol, a key component of membrane rafts and caveolae. To investigate that the effect of cholesterol depletion on the life cycle of ARV infection, treatment groups were set as follows: cells were treated with various concentrations of MβCD or nystatin prior to inoculation with virus. To further examine whether cholesterol plays an important role during the early step of the ARV life cycle, cells were treated with MβCD (3.2 mM) for 1 h at 37 °C, followed by supplementation with 50 mM cholesterol (Sigma) at different time points before, during, and after infection with ARV at an m.o.i. of 5. The drugs were kept in the medium throughout the infection. The cell lysates and supernatants of ARV-infected cells were collected 24 h post-infection for Western blot and viral titration, respectively. The level of ARV σC

protein was analyzed by Western blot. The progeny virus titer of ARV was determined by plaque assay.

For immunostaining, DF-1 cells in 6-cm cell culture dishes were treated with MβCD (3.2 mM) for 1 h at different time points before, during, and after infection with ARV at an m.o.i. of 5. The inhibitors were present during the whole infection period. ARV-infected cells were then fixed by methanol and stained with ARV σC antibody. Images were collected with a Zeiss LSM 510 META confocal microscope. To examine whether ARV uses a clathrin-dependent endocytotic pathway, other sets of DF-1 and Vero cells were also pretreated with various concentrations of CPZ and hypertonic sucrose medium for 1 h at 37 °C, followed by infection with ARV at an m.o.i. of 5. The drugs were also kept in the medium throughout the infection. To confirm that ARV does not use the clathrin-dependent endocytic pathway, we employed a physiological method, *i.e.* the use of hypertonic medium, to interfere with the clathrin pathway. We examined where transferrin uptake (a positive control) was inhibited by the hypertonic sucrose (100 mM) in medium. Furthermore, CPZ and sucrose were also used to block BEFV entry, which is known to use the clathrin-dependent pathway (a positive control).

Colocalization of ARV with Caveolin-1 by Immunostaining—DF-1 cells in 6-cm cell culture dishes were infected with ARV at an m.o.i. of 50 for 30 min. ARV-infected cells were then fixed by methanol and stained with ARV σC and caveolin-1 antibody. Images were collected with a Zeiss LSM 510 META confocal microscope with the pinhole set to achieve 1 airy unit. Colocalization of ARV σC with caveolin-1 was observed by confocal microscopy.

Knockdown of Caveolin-1 and Dynamin-2 Expression by siRNA—To explore whether phosphorylation of caveolin-1 was stimulated by ARV, first sets of Vero and DF-1 cells were infected with ARV at different multiplicities of infection and collected at 25 min post-infection. Second sets of Vero and DF-1 cells were infected with ARV at an m.o.i. of 5. Cells were infected with virus at 37 °C. Cell lysates were collected at indicated time points for examination of the expression level of caveolin-1 phosphorylation and dynamin-2 expression.

To define the role of caveolin-1 and dynamin-2 in the entry of ARV, DF-1 or Vero cells at 75% confluence were transfected with caveolin-1 gene-specific shRNA expression of pGFP-V-RS vector (caveolin-1 siRNA constructs in the pGFP-V-RS plasmid) and control siRNAs (29-mer noneffective scrambled pGFP-V-RS vector and pGFP-V-RS vector) (caveolin-1 mouse shRNA, TG500281, OriGene Co., Rockville, MD). Different sets of Vero and DF-1 cells were also transfected with dynamin-2 gene-specific shRNA expression of pGFP-V-RS vector (dynamin-2 siRNA constructs in the pGFP-V-RS plasmid) and control siRNAs (29-mer noneffective scrambled pGFP-V-RS vector and pGFP-V-RS vector) according to the manufacturer's instructions (dynamin-2 human shRNA, TG313406, OriGene Co.). Four different sets of caveolin-1 or dynamin-2 siRNA constructs in the pGFP-V-RS vector plasmid were tested in this study. Initial experiments revealed that the caveolin-1 siRNA construct GI356726 (CGTGTCAAGATTGACTTTGAAGATGTGA) and dynamin-2 siRNA construct GI353617 (CTACGGACCATCGGTGTCATCACCAAGCT) resulted in the most significant down-regulation of caveolin-1 and dynamin-2, respectively. Hence, these siRNA constructs were chosen for our further study. To transfect cells from each well on a 6-cm cell culture dish, 2 μl of TurboFect was mixed with 1 μg of plasmid in 100 μl of serum-free MEM for 20 min at room temperature. After 20 min of incubation, the TurboFect/plasmid mixture was added dropwise to each well. Cells were infected with ARV of at an m.o.i. of 5 at 24 h post-transfection. Cell lysates and supernatants of ARV-infected cells were harvested after 24 h post-infection and processed for Western blot and viral titration, respectively. The effect of caveolin-1 and dynamin-2 gene silencing in ARV entry was assessed by examination of the level of phosphorylated caveolin-1, dynamin-2, and σC protein as well as progeny virus titer of ARV. To further ensure the role of dynamin-2 in ARV entry, DF-1 or Vero cells were also pretreated with various concentrations of dynasore for 1 h and then infected with ARV at an m.o.i. of 5 for 24 h. The dynasore was present during the whole infection period.

Phosphorylation of Caveolin-1 and Dynamin-2 Expression Triggered by ARV via Activation of p38 MAPK and Src—To investigate whether activation of p38 MAPK and Src was triggered by ARV in the early stages of the virus life cycle, Vero and DF-1 cells were infected with ARV at an m.o.i. of 5 at 37 °C. The cell lysates were collected at different time points. Aliquots of cell lysates were examined for phosphorylation statuses of p38 MAPK and Src. The other two sets of DF-1 cells were treated with inhibitor SB202190 (5 μM) before and after ARV adsorption with an m.o.i. of 5 at 37 °C. The ARV-infected cells or cell lysates were collected at 24 h post-infection to assess cell syncytium formation or the level of σC, respectively. Another set of DF-1 cells was also treated with various concentrations of PP2 inhibitor for 1 h and then infected at an m.o.i. of 5. These inhibitors (SB202190 and PP2) were present during the whole infection. Infected cell lysates and supernatants of ARV-infected cells were collected at 24 h post-infection for examination of σC protein synthesis and viral titration, respectively.

Considering the finding that ARV induced activation of p38 MAPK and Src as well as phosphorylation of caveolin-1 and dynamin-2 expression, we then tested the hypothesis that Ras, p38 MAPK, and Src are upstream elements in the signaling cascades that induce the tyrosine phosphorylation of caveolin-1 and dynamin-2 expression. Suppression of phosphorylation of caveolin-1 and dynamin-2 expression by overexpression of Csk and DN mutants (p38 MAPK AF and Ras N17) as well as inhibitors (SB202190, PP2, and NSC23766) were carried out. Csk and DN mutants (p38 MAPK AF and Ras N17) were kindly provided by Professor W. L. Shih, National Pingtung University of Science and Technology, Taiwan. DF-1 cells were pretreated with inhibitors for 1 h and then infected with ARV at an m.o.i. of 5 for 25 min. The working concentrations of these inhibitors were as follows: 5 μM SB202190, 20 μM PP2, and 100 μM NSC23766. Cells treated with MβCD were also carried out to investigate whether cholesterol loss affects caveolin-1 phosphorylation and p38 MAPK and Src activation. All inhibitors used in this study were present during the whole infection period. In addition, another set of DF-1 cells were transfected with DN mutants and Csk expression plasmid for 24 h, respectively, and then infected with ARV S1133 at an m.o.i. of 5 for 25

min. Total cell lysates were subjected to Western blot using the respective antibodies for examination of the level of dynamin-2, p-caveolin-1 (Tyr^{14}), p-p38 MAPK, and p-Src.

To investigate whether caveolin-1 and dynamin-2 can mediate p38 MAPK and Src signaling pathways, DF-1 cells were also transfected with caveolin-1 siRNA or dynamin-2 siRNA for 24 h and then infected with ARV at an m.o.i. of 5 for 25 min. In addition, DF-1 cells were also pretreated with dynasore for 1 h and then infected with ARV at an m.o.i. of 5 for 25 min. Total cell lysates were subjected to Western blot using the respective antibodies for examination of the level of dynamin-2, p-caveolin-1 (Tyr^{14}), p-p38 MAPK, and p-Src.

Coimmunoprecipitation of Caveolin-1, Dynamin-2, p38 MAPK, Src, and Rac1—6-cm cell culture dishes were seeded with 1×10^6 DF-1 or Vero cells, and then the cells were cultured in media containing 2% FBS overnight. Cells were mock- or ARV-infected at an m.o.i. of 5 and then incubated for 30 min at 37 °C, after which the cells were incubated in maintenance media. The cells were washed twice in phosphate-buffered saline and scraped in 200 μl of lysis buffer. The cells were collected for immunoprecipitation by using the Catch and Release kit (Upstate Biotechnology; Lake Placid, NY) according to the manufacturer's protocol. About 500 μg of cellular proteins was incubated with 4 μg of rabbit anti-caveolin-1 polyclonal antibodies (Santa Cruz Biotechnology) at 4 °C overnight. The immunoprecipitated proteins were separated by SDS-PAGE followed by Western blotting, and then proteins were detected using the following antibodies: caveolin-1, dynamin-2, p38 MAPK, Src, and Rac1. Rabbit IgG was used as negative control. Experiments were also performed in reverse in which p38 MAPK, dynamin-2, or Rac1 antibodies were used for immunoprecipitation.

Rac1 Pulldown Assay—GTP-bound Rac1 was isolated from DF-1 cell lysates using a Rac1 activation assay kit (Millipore; San Diego) according to the manufacturer's protocol. In brief, DF-1 cells were grown in 6-cm cell culture dishes to 75% confluence, and the cells were then cultured in serum-free media overnight. DF-1 cells were infected with ARV at an m.o.i. of 5. Cell lysates were collected at the indicated times or 30 min for detection of GTP-Rac1. The cells were then rinsed with ice-cold PBS and lysed with Mg^{2+} lysis/wash buffer. After clarifying the cell lysates with glutathione-agarose and quantifying the protein concentrations, aliquots with equal amounts of proteins were incubated with Rac assay reagent at 4 °C for 45 min, using the GTPγS- and GDP-pretreated lysates as positive and negative controls. The precipitated GTP-bound Rac1 was then eluted in Laemmli reducing sample buffer, resolved in 10% SDS-PAGE, and immunoblotted using a specific antibody against Rac1.

To further examine whether Rac1 plays an important role during the early steps of ARV life cycle, DF-1 cells were also pretreated with NSC23766 at different time points before, during, and after ARV adsorption at 37 °C. Cell lysates and supernatants of ARV-infected cells were collected at 24 h post-infection for Western blot and viral titration, respectively. To examine whether p38 MAPK and Src are upstream inducers of Rac1, DF-1 cells were pretreated with various concentrations of inhibitors (SB202190 and PP2) for 1 h, respectively, and then infected with ARV at an m.o.i. of 5 for 30 min. Cell lysates were collected at 30 min post-infection for detection of GTP-Rac1. The inhibitors (NSC23766, SB202190, and PP2) used in this study were present during the whole infection period.

Inhibition of Microtubules and Rab5 by Means of Nocodazole and DN Mutants of Rab5—To investigate the potential role of microtubules in ARV productive infection, we assessed the effect of nocodazole or cytochalasin D on ARV infection. Vero and DF-1 cells were pretreated with different concentrations of nocodazole or cytochalasin D for 1 h and then infected with ARV at an m.o.i. of 5 for 24 h at 37 °C. To further examine whether microtubules play an important role during the early steps of the ARV life cycle, DF-1 cells were treated with nocodazole (1.25 μM) for 1 h at different time points before, during, and after absorption with ARV at an m.o.i. of 5. The inhibitors were present during the whole infection period.

To define the exact endosomal compartments traversed by endocytosed ARV, we used the DN mutants of Rab5 (S34N and Q79L) to study the requirement of transport to early endosomes in ARV infection. The Rab5 DN mutants were kindly provided by Professor Chi-Hung Lin, National Yang-Ming University, Taiwan. Cell lysates and supernatants of ARV-infected cells were collected at 24 h post-infection for Western blot and viral titration, respectively. The level of σC protein was analyzed by Western blot. The progeny virus titer of ARV was determined by plaque assay.

Determination of Endosomal Acidification Required for ARV Entry—DF-1 or Vero cells were pretreated with different concentrations of NH_4Cl, bafilomycin A1, and chloroquine for 1 h, followed by infection with ARV at an m.o.i. of 5 at 37 °C. The inhibitors were present during the whole infection period. Cell lysates and supernatants of ARV-infected cells were collected at 24 h post-infection for Western blot and viral titration, respectively. The cells were photographed at 24 h post-infection to assess cytopathic effect. The level of σC protein of ARV was analyzed by Western blotting. The progeny virus titer was determined by plaque assay.

Electrophoresis and Western Blot Assay—All the tested cells in 6-cm cell culture dishes were washed twice with phosphate-buffered saline, lysed in 60 μl of 2.5× Laemmli loading buffer, and then harvested by scraping and boiling for 10 min. Equal amounts of samples were separated by 10% SDS-PAGE and transferred to PVDF membranes. Expression level of individual protein was examined using respective antibodies, followed by the secondary antibodies (goat anti-mouse or goat anti-rabbit immunoglobulin G conjugated with HRP). After incubation with enhanced chemiluminescence (ECL Plus; Amersham Biosciences), the membranes were exposed to x-ray films (Eastman Kodak Co.). The intensity of each protein was calculated using Photocapt (Vilber Lourmat).

Statistical Analysis—All data were analyzed using independent sample *t* test and are expressed as averages of three independent experiments. *p* values of less than 0.05 were considered significant.

RESULTS

Cholesterol Is Required for an Early Stage of ARV Life Cycle— To determine whether more than one entry pathway was utilized

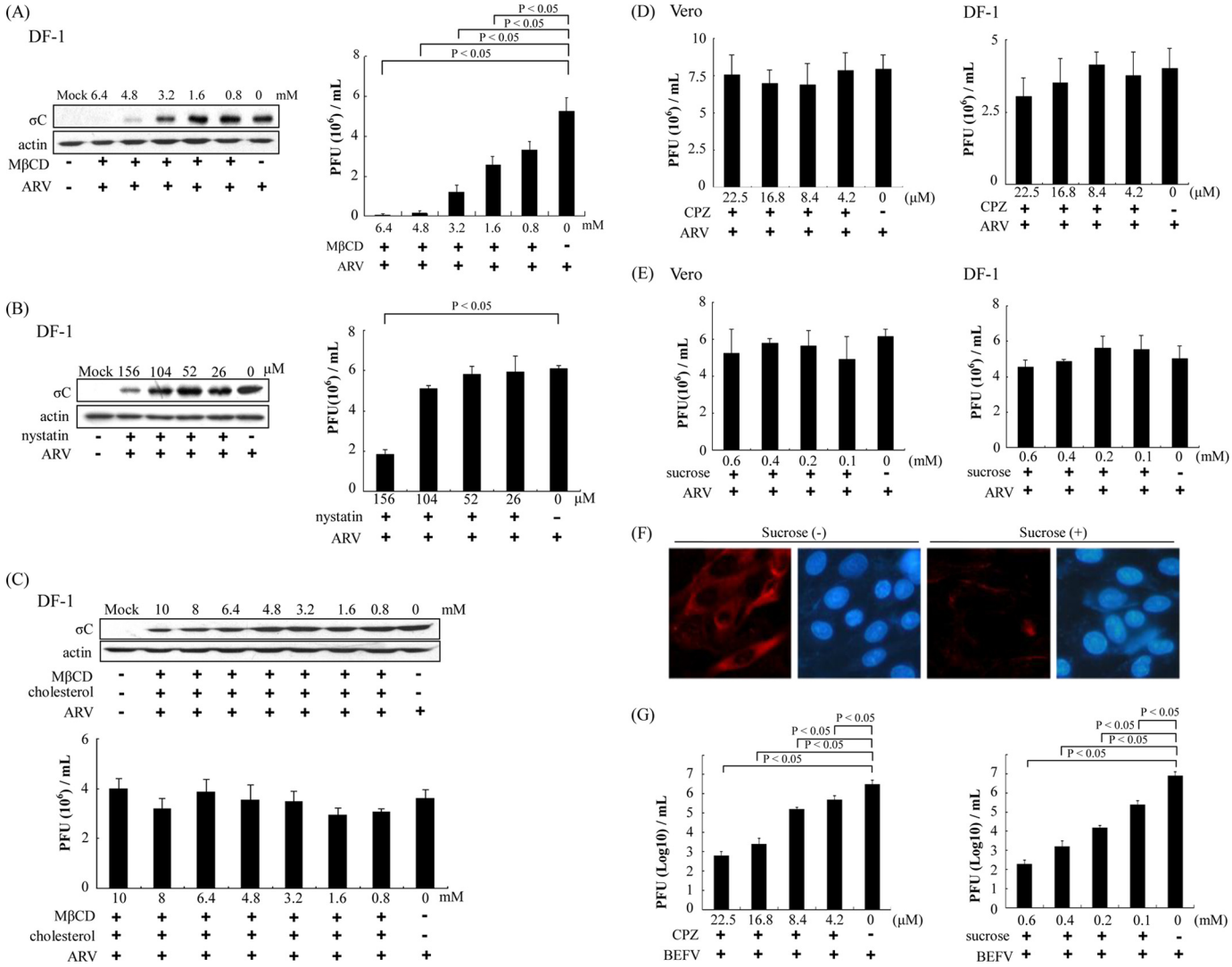

FIGURE 1. **Abrogation of lipid raft-dependent endocytosis blocks ARV infection.** DF-1 cells were pretreated with various concentrations of MβCD (*A*) or nystatin (*B*) for 1 h, followed by infection with ARV at an m.o.i. of 5 in the presence of MβCD or nystatin. *C,* various concentrations of MβCD plus cholesterol (50 μg/ml) were added to the medium before ARV adsorption at 37 °C. Cell lysates and supernatants of ARV-infected cells were collected 24 h post-infection for Western blot and viral titration, respectively. The level of σC protein of ARV was analyzed by Western blot. The progeny virus titer of ARV was determined by plaque assay. *D* and *E,* DF-1 and Vero cells were pretreated with various concentrations of CPZ and hypertonic sucrose medium for 1 h, followed by infection with ARV at an m.o.i. of 5. The supernatants of ARV-infected cells were collected 24 h post-infection. The progeny virus titer of ARV was determined by plaque assay. *F,* Vero cells were pretreated with 100 mM sucrose for 1 h; Alexa 568-labeled transferrin was bound and internalized, and uninternalized transferrin was removed by an acid wash. Fluorescence of Alexa 568-labeled transferrin is shown, along with a Hoechst 33258 counterstain for cell nuclei. *G,* Vero cells were pretreated with various concentrations of CPZ and hypertonic sucrose medium for 1 h, followed by infection with BEFV at an m.o.i. of 2. The supernatants of BEFV-infected cells were collected at the 24 h post-infection. The progeny virus titer of BEFV was determined by plaque assay. The result is from three triplicate experiments; *error bars* indicate the means ± S.D. The β-actin was used as an internal control for normalization.

by ARV, we examined the role of cholesterol in viral entry. To study the role of cholesterol in ARV infection, we used MβCD to deplete cholesterol in DF-1 cells for disruption of lipid raft. We tested the inhibitory effect of MβCD and nystatin in ARV-infected and mocked-infected DF-1 cells. The σC protein synthesis and progeny virus titer of ARV decreased dramatically in a dose-dependent manner in cells treated with MβCD (Fig. 1*A*). In a control experiment, we found that MβCD was unable to block BEFV entry in a dose-dependent manner (data not shown). The σC protein synthesis and progeny virus titer of ARV decreased to a lesser extent in a dose-dependent manner in cells treated with nystatin (Fig. 1*B*). To confirm the role of cholesterol, cholesterol (50 μg/ml) was supplemented after depletion of cellular cholesterol by MβCD for 1 h. The production of ARV was reversed by cholesterol supplementation, as demonstrated by the results seen with σC protein synthesis and progeny virus titer (Fig. 1*C*, *upper* and *lower panels*). These results reveal that the reduction of virus production was specifically due to the cholesterol depletion from host cells and that this effect was reversible. A similar trend was also seen in Vero cells. No significant reduction in virus production was observed in CPZ and sucrose-treated Vero or DF-1 cells (Fig. 1, *D* and *E*). In the control experiments, the transferrin internalization was significantly blacked by the presence of hypertonic sucrose medium, suggesting that hypertonic medium effectively blocks clathrin-mediated internalization (Fig. 1*F*). We also found that CPZ and sucrose were able to block BEFV entry, which is known to use the clathrin-dependent pathway (Fig. 1*G*). In this

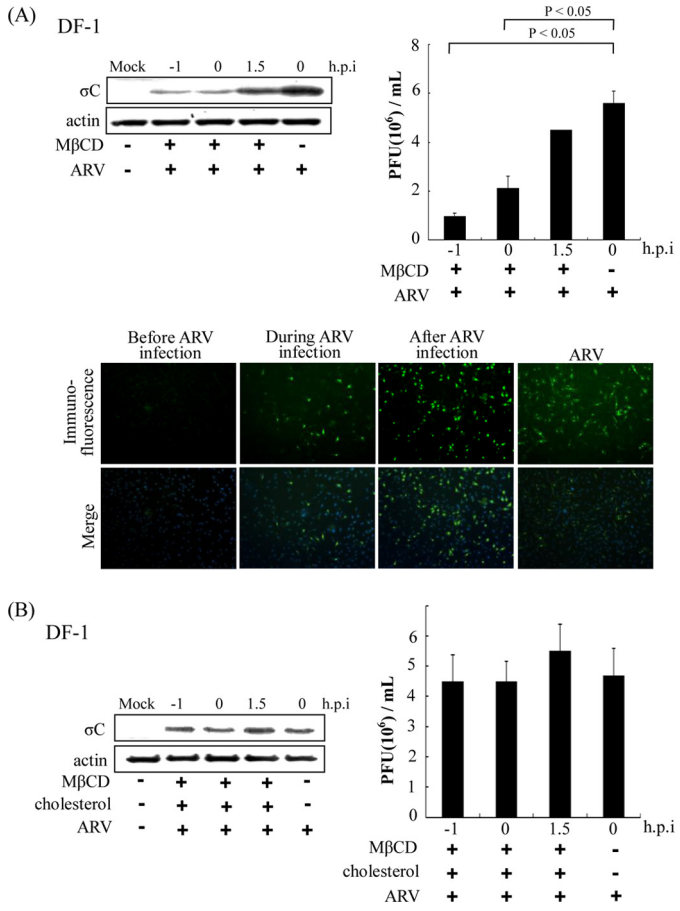

FIGURE 2. **Effects of MβCD are compensated by coincubation with cholesterol.** *A,* before, during, and after viral entry groups, MβCD (3.2 mM) was added to the medium during ARV (5 m.o.i.) adsorption at 37 °C. The cell lysates and supernatants of ARV-infected cells were harvested 24 h post-infection (*h.p.i.*) for Western blot and viral titration, respectively. Infected cells were also detected by immunofluorescence at 24 h post-infection using a monoclonal antibody against σC and then observed by confocal microscopy to visualize viral protein expression (green). The cell nuclei were stained with DAPI (blue). The results were merged using the program ImageJ. *B,* MβCD (3.2 mM) plus cholesterol (50 μg/ml) was added to the medium before, during, and after ARV adsorption at 37 °C. In the "after viral entry" group, MβCD (3.2 mM) plus cholesterol (50 μg/ml) was added to the medium after ARV (5 m.o.i.) adsorption at 37 °C. The cell lysates and supernatants of ARV-infected cells were harvested at 24 h post-infection for Western blot and viral titration, respectively. The result is from three triplicate experiments, *error bars* indicate the means ± S.D. The β-actin was used as an internal control for normalization.

study, neither CPZ nor a hypertonic medium (39) which contains sucrose inhibited ARV infection (Fig. 1, *D* and *E*), although MβCD was able to block virus entry in a dose-dependent manner. To investigate whether lipid rafts play a role in replication steps, cells were pretreated with MβCD (3.2 mM) before, during, and after ARV absorption for 1 h. When MβCD was added during or before the adsorption period, σC protein expression detected by Western blot or immunostaining as well as progeny virus titer of ARV decreased greatly (Fig. 2*A, upper* and *lower panels*); however, only a limited effect was observed on σC protein expression and virus production at the post-entry stage (Fig. 2*A*). The production of ARV was reversed by cholesterol supplementation before, during, and after the adsorption period, as demonstrated by the results seen with σC protein synthesis and progeny virus titer of ARV (Fig. 2*B*). These results suggested that the cholesterol present in host cytoplasmic membranes is important for early steps of ARV infection.

ARV Enters Host Cells via Caveolin-1-mediated Endocytosis—As shown in Fig. 3, *A* and *B*, the level of p-caveolin-1 (Tyr^{14}) upon ARV infection was elevated in a dose- and time-dependent manner in the early stage of the ARV life cycle. ARV induced an increase in caveolin-1 phosphorylation as early as 10 min post-infection in both Vero and DF-1 cells, attaining a maximal level at 30 min post-infection (Fig. 3*B*). Colocalization of ARV with caveolin-1 in ARV-infected DF-1 cells was also observed by confocal microscopy (Fig. 3*C*). We also used siRNA to specifically knock down the expression of caveolin-1. A significant reduction in the caveolin-1 and σC protein synthesis as well as progeny virus titer of ARV in the presence of caveolin-1 siRNA was seen in both Vero and DF-1 cells compared with the presence of control siRNAs (29-mer noneffective scrambled pGFP-V-RS vector and pGFP-V-RS vector) (Fig. 3*D, upper* and *lower panels*). Taken all findings together, these data reinforce the essential role of caveolin-1 during ARV entry into host cells.

ARV Infection Is Sensitive to Dynamin-2 Inhibition by Dynasore and Dynamin-2 siRNA—Dynamin is a GTPase required for the cellular membrane to pinch off endosomes from the plasma membrane and is necessary for clathrin- and caveola-mediated endocytosis and phagocytosis, but it is not required for macropinocytosis (11, 12). In this study, dynamin-2 was found to be unregulated in the early stage of the ARV life cycle. The level of dynamin-2 expression upon ARV infection was enhanced in a dose- and time-dependent manner in both Vero and DF-1 cells (Fig. 4, *A* and *B*). An increase in the level of dynamin-2 expression was seen as early as 10 min post-infection, attaining a maximal level at 30 min post-infection (Fig. 4*B*). As showed in Fig. 4*C*, dynasore significantly inhibited σC protein synthesis in a dose-dependent manner in DF-1 cells (Fig. 4*C, upper panel*). In the presence of dynasore, progeny virus titer of ARV was also decreased dramatically in a dose-dependent manner (Fig. 4*C, lower panel*). A similar trend was also seen in Vero cells. To further confirm our findings, an siRNA-mediated gene silencing against dynamin-2 was used. Vero and DF-1 cells transfected with dynamin-2 siRNA reduced dynamin-2 expression in comparison with Vero or DF-1 cells transfected with control siRNAs (29-mer noneffective scrambled pGFP-V-RS vector and pGFP-V-RS vector) (Fig. 4*D, upper* and *lower panels*). A significant decrease in the level of σC protein and progeny virus titer of ARV in the dynamin-2 siRNA-transfected cells was seen as compared with that of cells transfected with control siRNAs (Fig. 4*D, upper* and *lower panels*). Taken together, our results indicate that ARV entry into host cells takes place by caveolin-1-mediated endocytosis, which requires dynamin GTPase activity.

ARV Activates Src and p38 MAPK During the Very Early Stage of Life Cycle—More recently, we have demonstrated that activation of p38 MAPK and Src has been shown to up-regulate p53 upon ARV infection that is required for induction of apoptosis (33). In this study, we found that a significant increase in the phosphorylation level of Src and p38 MAPK in ARV-infected Vero and DF-1 cells was seen as early as 5 min post-infection, attaining a maximal level at 10 or 15 min post-infection, respectively (Fig. 5*A*). To explore which signaling

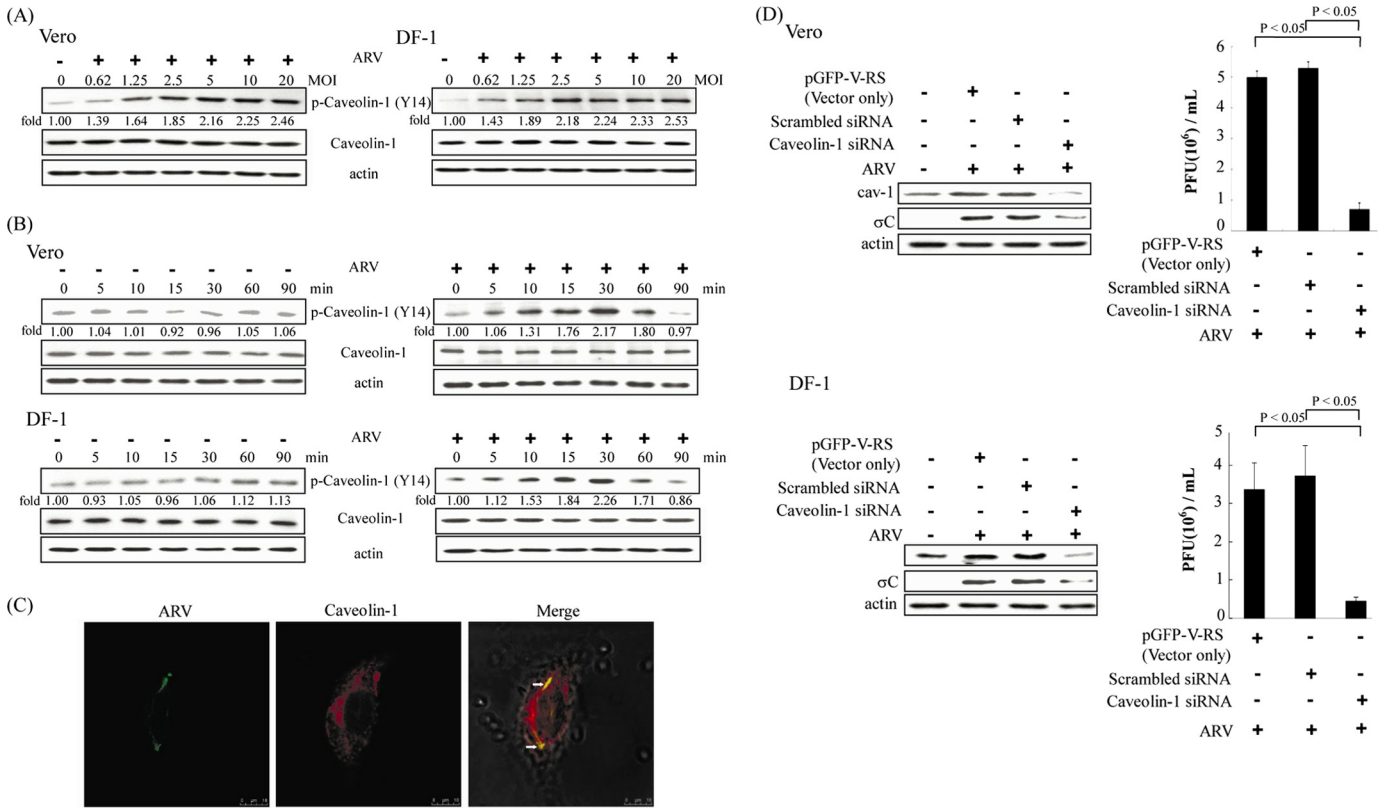

FIGURE 3. **ARV promotes the phosphorylation of caveolin-1 and is inhibited in cells transfected with siRNAs specific to caveolin-1.** *A,* Vero and DF-1 cells were infected with ARV at different multiplicities of infection (*MOI*). Cell lysates were collected at 25 min post-infection. *B,* Vero and DF-1 cells were infected with ARV at an m.o.i. of 5. Cell lysates were collected at the indicated times. Western blot was performed using the indicated antibodies against Tyr(P)[14]-caveolin-1. The level of phosphorylated caveolin-1 was quantitated by densitometric analysis using ImageJ and normalized to actin. *C,* colocalization of ARV with caveolin-1 was detected 30 min post-infection by immunofluorescence using antibody against σC or caveolin-1, respectively, and then observed by confocal microscopy. *Arrows* indicate the colocalization sites. The results were merged using the program ImageJ. *D,* Vero or DF-1 cells were transfected with caveolin-1 siRNA and control siRNAs (29-mer noneffective scrambled pGFP-V-RS vector and pGFP-V-RS vector) for 24 h and then infected with an m.o.i. of 5. Infected cells and supernatants of ARV-infected cells were collected at 24 h post-infection for Western blot and viral titration, respectively. Cell lysates were analyzed by Western blot using anti-caveolin-1, anti-σC, and anti-β actin antibodies. The progeny virus titer of ARV was measured by plaque assay. The result is from three triplicate experiments, *error bars* indicate the means ± S.D. The β-actin was served as an internal control for normalization. *p-*, phospho-.

molecules may involve ARV entry, we blocked p38 MAPK and Src using SB202190 and PP2 inhibitors, respectively. A significant decrease in cell syncytium formation and viral σC protein synthesis in the cells treated with SB202190 was seen before, during, and after absorption stage (Fig. 5, *B* and *C*). The expression level of σC protein and progeny virus titer of ARV in the cells treated with PP2 was decreased dramatically in a dose-dependent manner (Fig. 5*D*).

Inhibition of Ras, p38 MAPK, and Src Suppressed ARV-induced Caveolin-1 Phosporylation and Dynamin-2 Expression— DN mutants (Ras N17 and p38 MAPK AF), Csk, and inhibitors were used to investigate whether Ras, p38 MAPK, and Src signaling molecules are required for regulating caveolin-1 tyrosine 14 phosphorylation and dynamin-2 expression. The DN mutant expression and inhibitor working concentrations were not deleterious to the cells, as determined by measuring lactate dehydrogenase activity (data not shown). Overexpression of DN mutants and Csk in DF-1 cells was detected by Western blot (data not shown). To test whether there may be an upstream activator in our experimental system, the DN mutant of Ras N17 was ectopically expressed and then infected with ARV at an m.o.i. of 5. As shown in Fig. 6*A* (*right panel*), p-p38 MAPK was dramatically suppressed. Therefore, we conclude that ARV-induced p38 MAPK signaling activation is Ras-dependent. It is interesting to note that overexpression of DN mutants, Csk, and inhibitors abolished ARV-induced caveolin-1 tyrosine 14 phosporylation and dynamin-2 expression (Fig. 6, *A–C*) but not in DF-1 cells treated with NSC23766 (Fig. 6*D*). Therefore, the results strongly suggested that Ras, p38 MAPK, and Src but not Rac1 are required for regulating ARV-mediated caveolin-1 tyrosine 14 phosphorylation and dynamin-2 expression. As shown in Fig. 6*C*, p-p38 MAPK was not suppressed by PP2 inhibitor or overexpression of Csk, suggesting that Src is not the upstream inducer of p38 MAPK. These data are in agreement with our earlier report (33). It is also interesting to note that the expression level of p38 MAPK and Src in caveolin-1 or dynamin-2 siRNA-treated cell lysates was not significantly altered (Fig. 6*E*). It was found that cholesterol loss was unable to affect p38 MAPK and Src activation but down-regulated phosphorylation of caveolin-1 (Fig. 6*F*, *left panel*). In addition, dynamin inhibition by dynasore was also done to examine cells inhibited by dynasore for virus-dependent phosphorylation of caveolin-1, p-p38 MAPK, and p-Src. Similar results were obtained as dynamin-2 siRNA treatment (Fig. 6*F*, *right panel*). These results suggested that neither caveolin-1 nor dynamin-2 can regulate p38 MAPK and Src signaling pathways. Our results

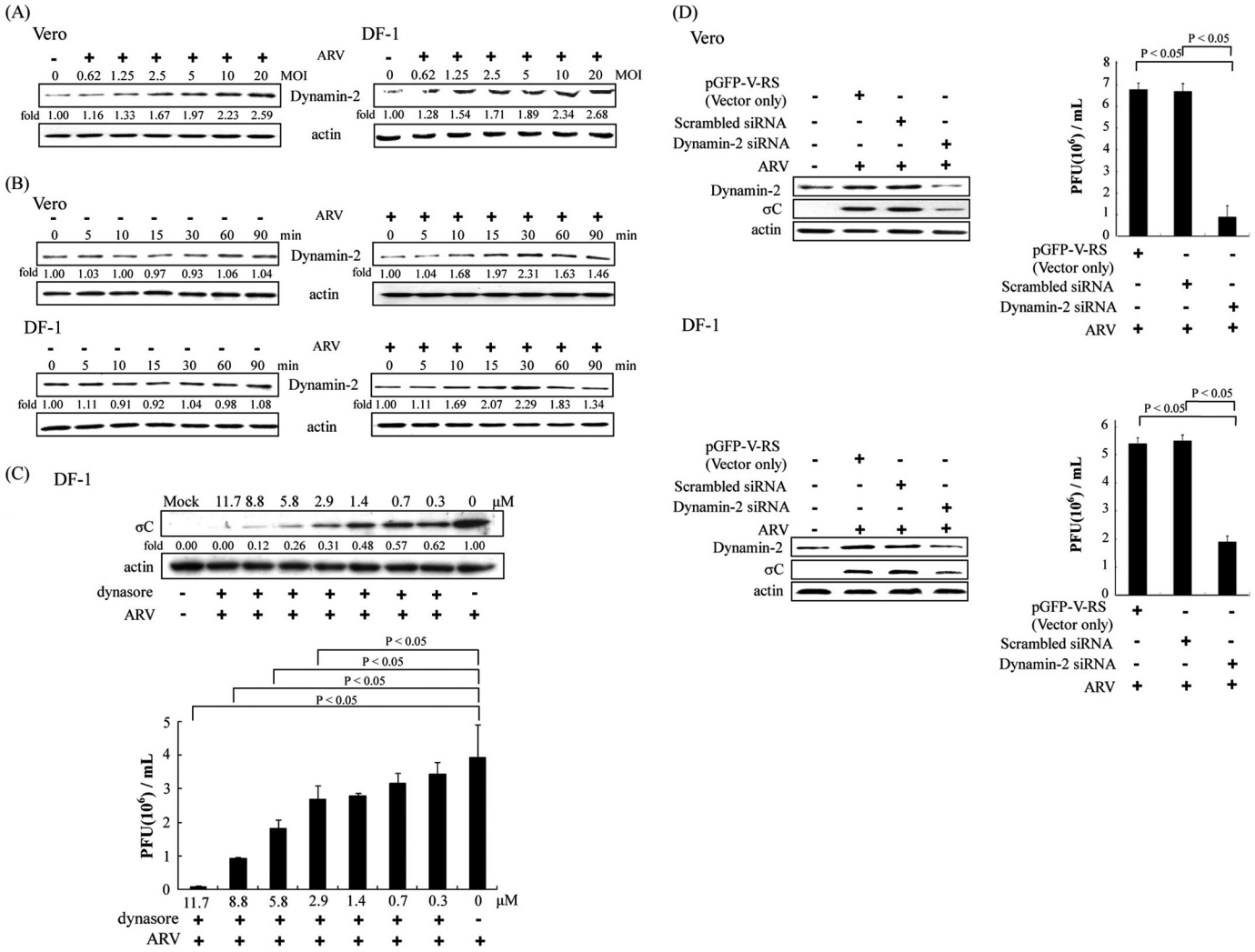

FIGURE 4. **ARV infection was impaired by inhibition of dynamin activity.** *A,* Vero and DF-1 cells were infected with ARV at different multiplicities of infection (*MOI*). Cell lysates were collected at 25 min post-infection. *B,* Vero and DF-1 cells were infected with ARV at an m.o.i. of 5. Cell lysates were collected at the indicated times. Western blot was performed using antibodies against dynamin-2. The expression level of dynamin-2 was quantitated by densitometric analysis using ImageJ and normalized to actin. *C,* DF-1 cells were treated with different concentrations of dynasore for 1 h and then infected with ARV at an m.o.i. of 5. Infected cells and supernatants of ARV-infected cells were collected at 24 h post-infection for Western blot and viral titration, respectively. Cell lysates were analyzed by Western blot using ARV σC antibody, with β-actin as an internal control. The level of σC protein was quantitated by densitometric analysis using ImageJ and normalized to actin. The progeny virus titer of ARV was determined by plaque assay. The result is from three triplicate experiments, *error bars* indicate the means ± S.D. *D,* Vero or DF-1 cells were transfected with dynamin-2 siRNA (pGFP-V-RS) and control siRNAs (29-mer noneffective scrambled pGFP-V-RS vector and pGFP-V-RS vector) for 24 h and then infected with an m.o.i. of 5. Infected cells and supernatants of ARV-infected cells were collected at 24 h post-infection for Western blot and viral titration, respectively. Cell lysates were analyzed by Western blot using anti-dynamin-2, anti-σC, and anti-β-actin antibodies. The β-actin was served as an internal control for normalization. The virus titer was determined by plaque assay. The result is from three triplicate experiments, *error bars* indicate means ± S.D..

further suggested that signaling occurs before uptake, and uptake depends on signal activation. Similar results were also observed in Vero cells.

p38 MAPK and Src Are Associated with Caveolin-1 and Dynamin-2—As shown in supplemental Fig. 1*A*, immunoprecipitation of caveolin-1 using anti-caveolin-1 antibody and Western blotting with caveolin-1, dynamin-2, p38 MAPK, and Src antibodies revealed that these proteins are associated. In reciprocal experiments in which cell lysates were immunoprecipitated with p38 MAPK or dynamin-2 antibody, caveolin-1, dynamin-2, p38 MAPK, and Src but not Rac1, were detected by Western blotting (supplemental Fig. 1, *B* and *C*). In reciprocal experiments in which cell lysates were immunoprecipitated with Rac1 antibody, caveolin-1, dynamin-2, and p38 MAPK were not detected by Western blot (supplemental Fig. 1*D*), suggesting that Rac1 does not interact with these proteins. As a control, there was an absence of caveolin-1, dynamin-2, p38 MAPK, and Src coimmunoprecipitation when normal rabbit IgG was used as the precipitating antibody. In an attempt to detect the phosphorylated Src and p38 MAPK, however, we only detected their unphosphorylated total proteins and not the phosphorylated form of proteins in our experimental conditions.

Activation of p38 MAPK and Src by ARV Is Required for Activation of Rac1—Suppression of ARV-activated Rac1 by NSC23766 (100 μM) in DF-1 cells was seen (Fig. 7*A*). Rac1 triggered by ARV occurred as early as 10 min post-infection, attaining a maximal level at 30 min post-infection (Fig. 7*B, upper*

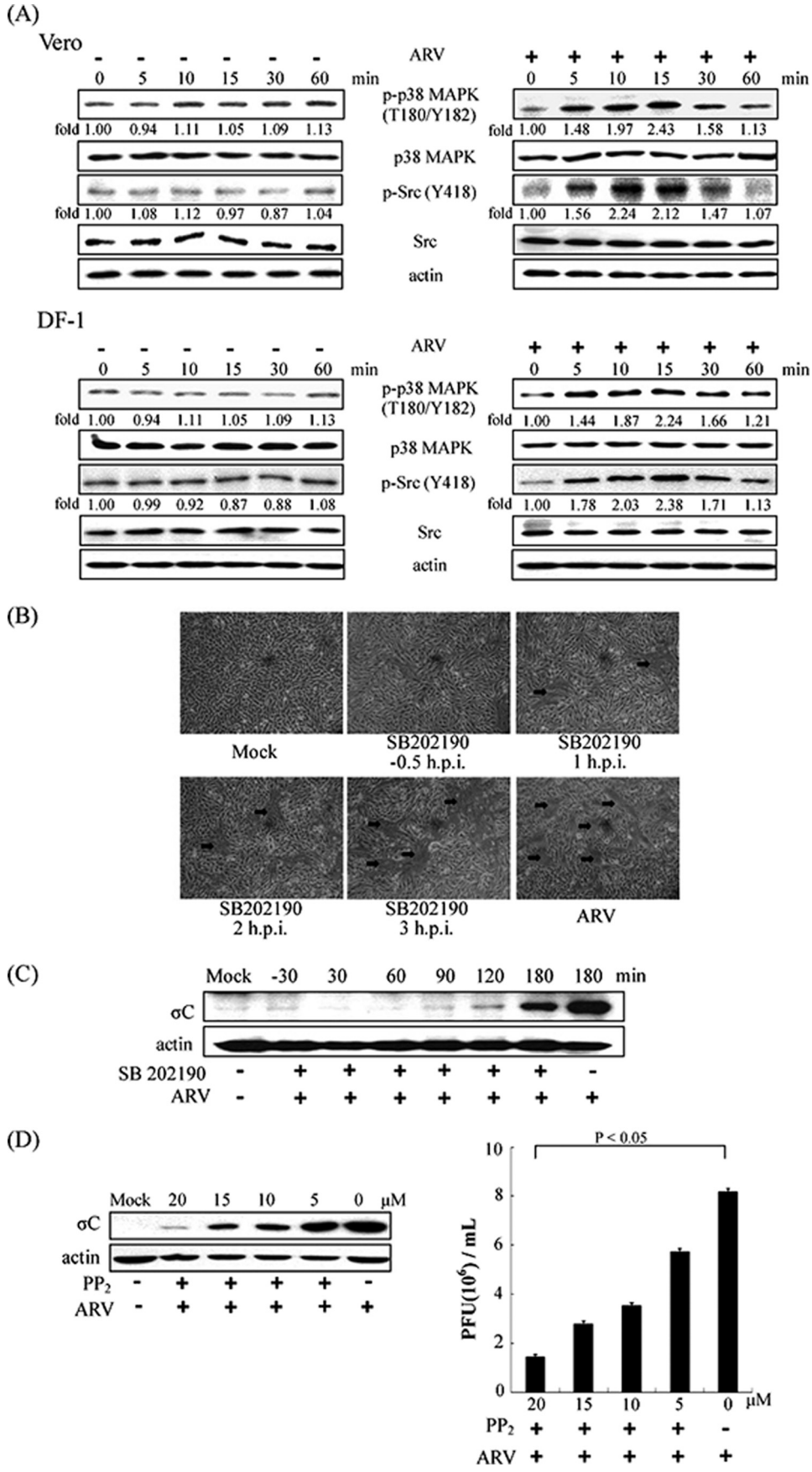
(A)
Vero
ARV
0 5 10 15 30 60 min
p-p38 MAPK (T180/Y182)
fold 1.00 0.94 1.11 1.05 1.09 1.13
fold 1.00 1.48 1.97 2.43 1.58 1.13
p38 MAPK
p-Src (Y418)
fold 1.00 1.08 1.12 0.97 0.87 1.04
fold 1.00 1.56 2.24 2.12 1.47 1.07
Src
actin
DF-1
fold 1.00 0.94 1.11 1.05 1.09 1.13
fold 1.00 1.44 1.87 2.24 1.66 1.21
fold 1.00 0.99 0.92 0.87 0.88 1.08
fold 1.00 1.78 2.03 2.38 1.71 1.13
(B)
Mock
SB202190 -0.5 h.p.i.
SB202190 1 h.p.i.
SB202190 2 h.p.i.
SB202190 3 h.p.i.
ARV
(C)
Mock -30 30 60 90 120 180 180 min
σC
actin
SB 202190
ARV
(D)
Mock 20 15 10 5 0 μM
σC
actin
PP2
ARV
P < 0.05
PFU(10^6) / mL
20 15 10 5 0 μM
PP2
ARV

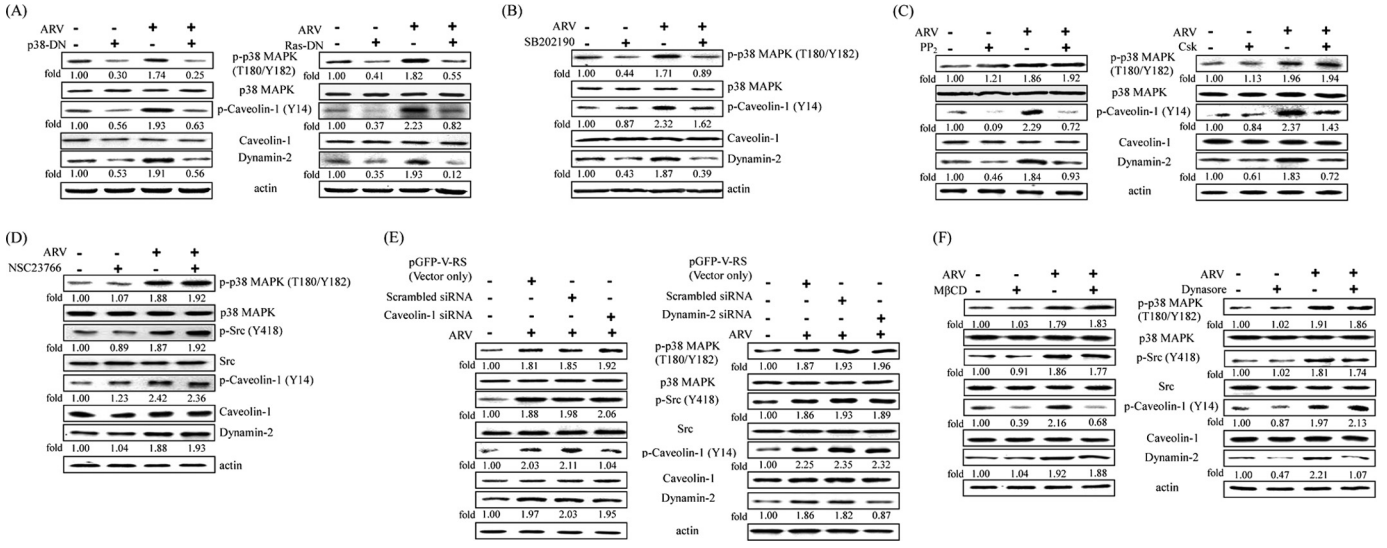

FIGURE 6. **Inhibition of ARV-induced caveolin-1 phosphorylation and dynamin-2 by inhibitors as well as overexpression of Csk and DN mutants.** Suppression of phosphorylation of Tyr(P)[14]-caveolin-1 and dynamin-2 expression by overexpression of DN mutants (Ras N17 and p38 MAPK AF) (*A*) and Csk (*C*) as well as inhibitors SB202190 (*B*), PP2 (*C*), and NSC237662 (*D*). DF-1 cells were preincubated with inhibitors for 1 h and then infected with ARV at an m.o.i. of 5. Other sets of DF-1 cells were transfected with DN mutants and Csk expression plasmids for 24 h, respectively, and then infected with ARV at an m.o.i. of 5. Cell lysates were collected at 25 min post-infection and immunoblotted with respective antibodies. *E,* DF-1 cells were transfected with caveolin-1 or dynamin-2 siRNA for 24 h, respectively, and then infected with ARV at an m.o.i. of 5 for 25 min. *F,* DF-1 cells were pretreated with MβCD or dynasore for 1 h, respectively, and then infected with ARV at an m.o.i. of 5 for 25 min. Total cell lysates were subjected to Western blot using the respective antibodies, respectively. β-Actin was included as an internal control. The level of respective protein was quantitated by densitometric analysis using ImageJ and normalized to actin. The values shown are the means of three independent experiments. *p-*, phospho-.

panel). As shown in Fig. 7*B* (*lower panel*), viral σC protein synthesis and progeny virus titer of ARV in the DF-1 cells treated with NSC23766 (100 μM) decreased dramatically before absorption stage, suggesting that Rac1 plays an important role in the early stage of virus life cycle. Upon Rac1 inhibition, the ability of ARV to induce cell syncytium formation was also inhibited (22), as seen in SB202190-treated cells (Fig. 5*C*). Similar results were also obtained in Vero cells. The level of GTP-Rac1 was greatly decreased by inhibitors SB201290 and PP2 in a dose-dependent manner (Fig. 7*C*), suggesting that p38 MAPK and Src are upstream inducers of Rac1. Similar trend was also seen in Vero cells.

Microtubules and Small GTPase Rab5 Are Required for ARV Productive Infection—Microtubules contribute to regulation of cargo trafficking within endosomal compartments and serve as scaffolding structures for a variety of cellular proteins, including Rab5 (40). Consistent with this, microtubules have been reported in cell entry of several viruses (41). To examine the potential role of microtubules in ARV productive infection, we assessed the effect of nocodazole on ARV infection. In this study, treatment of DF-1 cells with nocodazole (1.25 μM) before and during absorption reduced the σC protein synthesis or progeny virus titer of ARV up to 9-fold (Fig. 8*A*). Treatment of Vero and DF-1 cells with various concentrations of nocodazole reduced significantly progeny virus titer of ARV (Fig. 8*B*). Actin cytoskeleton has been reported in cell entry of several viruses (38). To determine whether actin cytoskeleton also played a role during the early stage of the ARV life cycle, DF-1 and Vero cells were pretreated with cytochalasin D at various concentrations for 1 h prior to ARV absorption. It was found that cytochalasin D did not exert an adverse effect on ARV replication (Fig. 8*C*), suggesting that actin filaments are not necessary for ARV productive infection. Taken together, we demonstrated that microtubules, but not actin dynamics, play an important role in the early stage of ARV life cycle.

Rab5 GTPase is the key regulator of transport to early endosomes (42, 43) and blockage of Rab5 has been widely utilized to study viral entry (35, 44). To identify the exact endosomal compartment(s) traversed by endocytosed ARV, overexpression of the DN mutants of Rab5 (S34N and Q79L) was carried out to examine the requirement of transport to early endosomes in the entry of ARV. Overexpression of DN mutants of Rab5 reduced the σC protein synthesis and progeny virus titer of ARV up to 10-fold (Fig. 8*D*).

ARV Infection Requires a Low pH Compartment—Based on the observation that ARV enters the host cells via caveolin-

FIGURE 5. **Time course of ARV activating the phosphorylation of p38 MAPK and Src and their effects on ARV multiplication.** *A,* Vero and DF-1 cells were infected with ARV at an m.o.i. of 5, and cell lysates were collected at the indicated times. Aliquots of cell lysates were examined for phosphorylation statuses of p38 MAPK and Src (Tyr^{418}). Total p38 MAPK, Src, and β-actin were probed as loading controls. Western blot was performed using antibodies against p38 MAPK and Src. The expression level of p38 MAPK and Src was analyzed by Western blot. The level of p-p38 MAPK and p-Src was quantitated by densitometric analysis using ImageJ and normalized to actin. Similar results were obtained in three independent experiments. *B,* DF-1 cells were treated with inhibitor SB202190 (5 μM) before and after ARV adsorption with an m.o.i. of 5. The cells were photographed at 24 h post-infection (*h.p.i.*) to assess cell syncytium formation. *Arrows* indicate the sites of cell syncytium formation. *C,* DF-1 cells were treated with inhibitor SB202190 (5 μM) before and after ARV adsorption with an m.o.i. of 5. Cell lysates were collected at 24 h post-infection. The level of σC protein of ARV was examined by Western blot, with β-actin as an internal control. *D,* DF-1 cells were treated with various concentrations of PP2 inhibitor for 1 h and then infected with an m.o.i. of 5. The cell lysates and supernatants of ARV-infected cells were collected 24 h post-infection for examination of σC protein synthesis and progeny virus titer, respectively. Actin was included here as an internal control. The values shown are the means of three independent experiments, and the *error bars* indicate means ± S.D. *p-*, phospho.

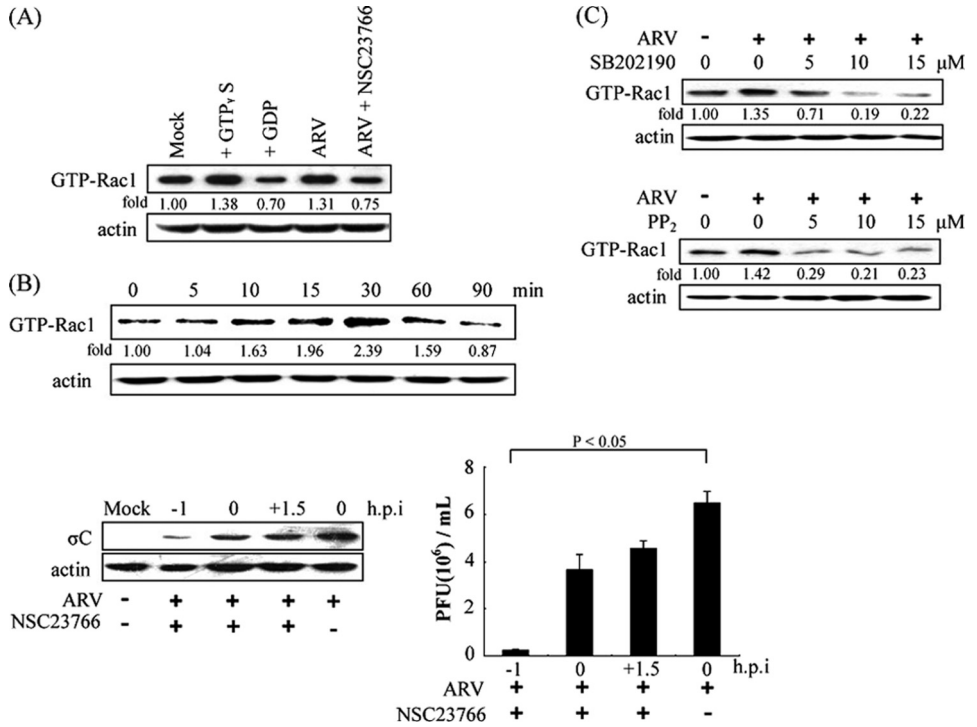

FIGURE 7. **ARV-activated Rac1 through activation of p38 MAPK and Src.** DF-1 cells were grown in 6-cm^2 cell culture dishes to 75% confluence, and then the cells were cultured in serum-free media overnight. Pulldown assay for GTP-Rac1 was performed. *A,* DF-1 cells were infected with ARV at an m.o.i. of 5, and then cell lysates were collected at 30 min post-infection for Western blot using the GTPγS- and GDP-pretreated lysates as positive and negative controls. *B,* DF-1 cells were infected with ARV at an m.o.i. of 5 and collected at indicated times for detection of the expression level of GTP-Rac1. Another set of experiments, DF-1 cells were treated with inhibitor NSC23766 (100 μM) before, during, and after ARV adsorption with ARV at an m.o.i. of 5. The cell lysates and supernatants were collected at 24 h post-infection for examination of the level of σC protein and determination of progeny virus titer of ARV, respectively. β-Actin was probed as a loading control. The values shown are the means of three independent experiments, and the *error bars* indicate means ± S.D. *C,* DF-1 cells were pretreated with different concentrations of inhibitors SB202190 and PP2, respectively, for 1 h and then infected with ARV at an m.o.i. of 5. Aliquots of cell lysates were collected at 30 min post-infection for examination of the expression level of GTP-Rac1. The level of GTP-Rac1 was quantitated by densitometric analysis using ImageJ and normalized to actin. Similar results were obtained in three independent experiments.

mediated and dynamin-dependent endocytosis, we next investigated whether ARV infection needs the acidic environment of the endosomal compartment. We first tested the requirement of low endosomal pH for ARV entry using the endosomotropic weak base NH_4Cl, because it instantaneously raises the pH of cellular vacuolar compartments. NH_4Cl strongly inhibited cell syncytium formation induced by ARV (supplemental Fig. 2*A*, *left panel*) and showed a marked inhibitory effect on progeny virus production in a dose-dependent manner (supplemental Fig. 2*A*, *right panel*). We further tested the involvement of acidic pH in the ARV entry by inhibition of vacuolar ATPase. Incubation of cells with the bafilomycin A1 resulted in a strong inhibitory effect on σC protein synthesis (supplemental Fig. 2*B*, *left panel*) and progeny virus production (supplemental Fig. 2*B*, *right panel*) in a dose-dependent manner, whereas chloroquine had a moderate effect on virus production (supplemental Fig. 2*C*), confirming the requirement of low endosomal pH for infection. A similar trend was also seen in DF-1 cells. The results obtained using several inhibitors of endosome acidification revealed that ARV uses a low pH-dependent entry pathway (17, 36).

DISCUSSION

The use of chemicals to inhibit or modify the cellular process has provided important insights into the early events of viral infections. It was an extension of earlier studies by our laboratory in which it was discovered that p38 MAPK and Src signaling pathways triggered by ARV that are beneficial for ARV replication and apoptosis induction (31, 33). In this study, the use of a panel of chemical inhibitors, DN mutants together with siRNAs targeting caveolin-1 and dynamin-2 to characterize ARV entry into host cells revealed that ARV uses a cholesterol and caveolin-1-mediated and dynamin-2-dependent endocytosis that requires activation of Ras, p38 MAPK, and Src signaling pathways. The participation of the microtubules and small GTPase Rab5 in regulating transport to the early endosome was also found in ARV entry. To my knowledge, this is the first report to elucidate that Ras-p38 MAPK and Src signaling pathways as well as microtubules and small GTPase Rab5 play an important role in ARV entry and replication.

MβCD that disrupts the cholesterol-rich microdomain results in the inhibition of both the caveolin-dependent endocytosis and caveola-independent lipid raft-dependent endocytosis (45, 46). Previous reports suggest that the cholesterol-rich lipid rafts are involved in distant steps of the life cycle in a number of enveloped and even nonenveloped viruses (17, 45–48). The nonstructural proteins of flaviviruses (DEN-2 and Japanese encephalitis virus) were reported to be associated with detergent-resistant membranes, and their replication complex may be located in the lipid raft structures of infected cell membranes (49). In the case of human immunodeficiency virus

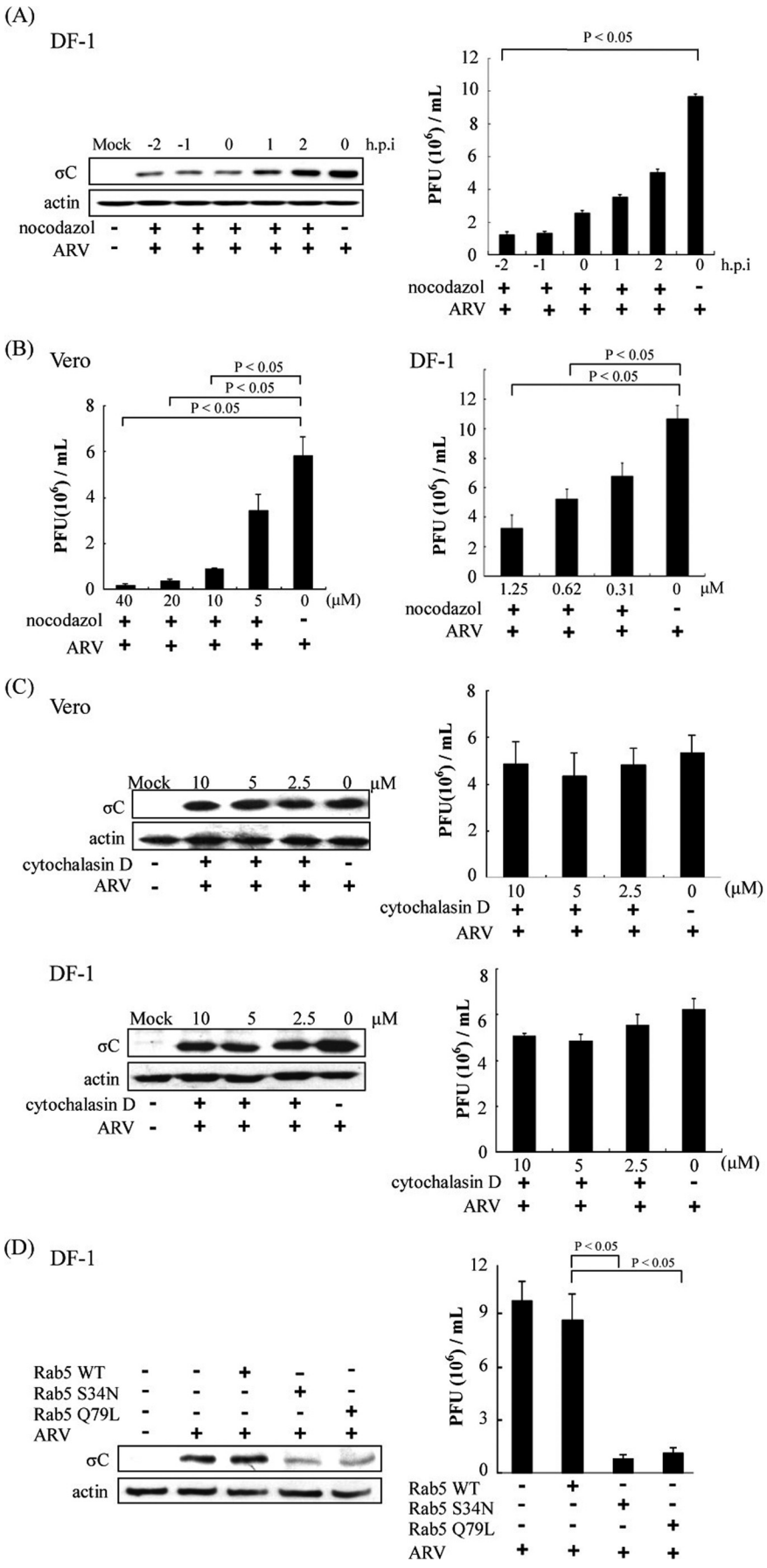
(A)
DF-1
Mock -2 -1 0 1 2 0 h.p.i
σC
actin
nocodazol - + + + + + -
ARV - + + + + + +
P < 0.05
PFU (10^6) / mL
-2 -1 0 1 2 0 h.p.i
nocodazol + + + + + -
ARV + + + + + +
(B)
Vero
P < 0.05
P < 0.05
P < 0.05
PFU(10^6) / mL
40 20 10 5 0 (μM)
nocodazol + + + + -
ARV + + + + +
DF-1
P < 0.05
P < 0.05
PFU (10^6) / mL
1.25 0.62 0.31 0 μM
nocodazol + + + -
ARV + + + +
(C)
Vero
Mock 10 5 2.5 0 μM
σC
actin
cytochalasin D - + + + -
ARV - + + + +
PFU(10^6) / mL
10 5 2.5 0 (μM)
cytochalasin D + + + -
ARV + + + +
DF-1
Mock 10 5 2.5 0 μM
σC
actin
cytochalasin D - + + + -
ARV - + + + +
PFU (10^6) / mL
10 5 2.5 0 (μM)
cytochalasin D + + + -
ARV + + + +
(D)
DF-1
Rab5 WT - - + - -
Rab5 S34N - - - + -
Rab5 Q79L - - - - +
ARV - + + + +
σC
actin
P < 0.05
P < 0.05
PFU (10^6) / mL
Rab5 WT - + - -
Rab5 S34N - - + -
Rab5 Q79L - - - +
ARV + + + +

infection, cholesterol depletion affects virus entry, thereby reducing the viral infectivity (45). Furthermore, it has been implicated that hepatitis C virus RNA replication occurs on a lipid rafts recruited from the intracellular membranes (48). In this work, our results reveal that the plaque-forming ability of ARV was enhanced by the cholesterol supplementation. However, the effect of this phenomenon was reversed for some viruses, such as DEN-2 and Japanese encephalitis virus, as cholesterol greatly blocked their infectivity (49). Further deciphering any role of membrane rafts in the replication cycle of ARV and experiments elucidating the underlying molecular mechanisms or evidence for the specific raft-targeting motif interacting with the viral proteins are now in progress. Thi study first demonstrated the importance of membrane cholesterol for ARV entry. Previous studies suggested that cholesterol plays an important role in the formation of caveolae and that the N-terminal end of the caveolin scaffolding domain of caveolin-1 contains a conserved serine residue mediating cholesterol binding (50). In this study, cholesterol depletion by pretreatment of cells with MβCD inhibited the entry and production of ARV, which probably interfere with the formation of caveolae or acts by either changing the receptor levels on the cell surfaces or preventing virus binding to the target cells. The inhibitory effect of MβCD was reversed by replenishment of cholesterol, suggesting that cellular cholesterol levels are tightly controlled by biosynthesis, efflux, and influx of cholesterol into cells. The membrane association may provide a structural framework for replication, with the advantages of increasing the local concentrations of necessary components and protecting the viral RNA molecules. In this study, we provide evidence demonstrating that disruption of lipid raft formation by either MβCD or nystatin decreased ARV infection, mainly at viral entry and a lesser extent at intracellular replication step(s). However, MβCD was unable to block BEFV entry that is known to use the clathrin-dependent pathway (as a control).[3] Therefore, elucidation of the importance of rafts in the ARV life cycle should help to define precisely the main events of the ARV infectious cycle and to provide some clues to develop new antiviral strategies.

In this study, we discovered up-regulation of both caveolin-1 and dynamin-2 by ARV via activation of p38 MAPK and Src signaling pathways in the very early stage of the virus life cycle. To examine more precisely the role of caveolin-1- and dynamin-2-mediated endocytosis in ARV entry, we utilized caveolin-1 and dynamin-2 siRNAs to disrupt endocytic pathways. By silencing caveolin-1 and dynamin-2, ARV infection was specifically reduced. By means of dynamin-2 siRNA and dynasore to disrupt dynamin-dependent endocytosis, even though the assays are different, both led to similar conclusions, indicating that ARV entering cell is dynamin-2-dependent. The involvement of dynamin-2 and the low pH dependence in ARV infection suggest that caveolin-1-mediated endocytosis is the pathway for ARV entry. Colocalization of ARV virions with caveolin-1 as demonstrated by confocal microscopy during the very early stage of the life cycle and the reduction of infection by silencing the caveolin-1 gene further support our conclusion. These results restrict the studies to the caveolin-1-mediated and dynamin-2-dependent routes by endocytosis.

Viral infections are known to activate various cellular signaling pathways to facilitate replication. An increasing amount of information has demonstrated that many viruses activate the p38 MAPK pathway to augment their efficient replication (51–55). To this end, although in our earlier study we have demonstrated that p38 MAPK activation is beneficial for ARV replication (31), its precise role in regulating ARV entry and replication remains elusive so far. Thus, we attempted to elucidate the p38 MAPK and Src signaling pathways by characterizing the cross-talk with cellular proteins caveolin-1 and dynamin-2. The requirement of the caveolin-1-mediated and dynamin-2-dependent endocytic pathway as well as concomitant activation of p38 MAPK and Src signal pathways to assist ARV entry is first demonstrated. By means of DN mutants and specific inhibitors to Ras, p38 MAPK and Src signaling allow us to dissect the individual role of these pathways in ARV entry. Here, we provide evidence demonstrating a novel role for p38 MAPK and Src signaling in exerting positive effects on ARV entry and productive infection. Inhibition of p38 MAPK and Src was associated with the marked reduction of the dynamin-2 expressions and phosphorylated level of caveolin-1, along with the apparent reduction of viral protein synthesis and viral progeny titer, suggesting that multiple signaling pathways triggered by ARV play a crucial role in mediating ARV entry and replication. This hypothesis is further supported by our results that p38 MAPK and Src are associated with caveolin-1, the major marker of caveolae. A number of signaling proteins interact with the binding motif of caveolin-1 scaffolding domain (56). Hence, the signaling triggered by ARV may interact with the scaffolding domain of caveolin-1. Based on our data, we propose that the interaction between caveolin-1 and dynamin-2 and these signaling proteins is crucial for ARV entry. As several kinases are inextricably linked to endocytic machinery (57), the interaction of p38 MAPK and Src with caveolin-1 may also be important in bringing together components of the endocytic machinery mediating ARV entry and subsequent replication. Aside from their role in mediating ARV entry, both p38 MAPK and Src facilitate Rac1 activation. The well studied members of the Rho-GTPase family are RhoA, Cdc42, and Rac1 (58–60). Besides its role in cytoskeletal regulation, Rho-GTPases also

[3] W. R. Huang, Y. C. Wang, P. I. Chi, L. Wang, C. Y. Wang, C. H. Lin, and H. J. Liu, unpublished data.

FIGURE 8. **Inhibition of ARV infection by the disrupted microtubule assemble and repression of Rab5.** *A,* DF-1 cells were pretreated with nocodazole (1.25 μM) or with DMSO as a mock control for 1 h at different time points before, during, and after ARV absorption at an m.o.i. of 5. The cell lysates and supernatants of ARV-infected cells were collected at 24 h post-infection (*h.p.i.*) for viral titration, respectively. *B* and *C,* Vero or DF-1 cells were treated with various concentrations of nocodazole (*B*) or cytochalasin D (*C*) for 1 h and then infected with ARV at an m.o.i. of 5. The cell lysates and supernatants of ARV-infected cells were collected at 24 h post-infection for Western blot and viral titration, respectively. *D,* DF-1 cells transfected with DN mutants of Rab5 (S34N and Q79L) for 24 h and then infected with ARV at an m.o.i. of 5 for 24 h. Cells lysates and supernatants were collected for Western blot and viral titration, respectively. The level of σC protein was examined by Western blot, with β-actin as an internal control. The progeny virus titer of ARV was determined by plaque assay. The result is from triplicate experiments, and the *error bars* indicate means ± S.D.

participate in a variety of cellular processes (58–62). In this study, activation of Rac1 is required for ARV productive infection, because inhibition of Rac1 or its upstream signals strongly reduced cell syncytium formation and virus production. It is interesting to note that although activation of Rac1 is required for ARV productive infection, the actin modulator Rac1 did not regulate actin in our case. In this study, we have demonstrated that p38 MAPK and Src play important roles in mediating virus entry and cell syncytium formation that is beneficial for virus replication. Taking all findings together, by orchestrating the signaling cascades, ARV may create a better intracellular environment to facilitate its productive infection.

Modulation of cytoskeleton organization is important for efficient replication of several viruses (63–65). Nef protein in HIV virions functions to allow the viral genome to penetrate the cortical actin network beneath the cytoplasmic membrane (64). The VP40 protein of Ebola virus directly enhances tubulin polymerization, suggesting that microtubules may play an important role in the virus life cycle (65). In the case of Junin virus, cytoskeleton is important for the initiation of the assembly and budding processes at the plasma membrane. Inhibition of assembly of cytoskeletons by chemicals can dramatically reduce viral protein expression or virus production (63). In this study, microtubule disruption impaired ARV infectivity. Because early endosomal transport requires microtubules, it is very likely that ARV requires transport from early to late endosomes for infection. Because microtubule disruption also affects multiple cellular functions, the specificity of the requirement of early endosomal compartments for the completion of the life cycle of ARV was also examined. Data obtained in this study provide evidence demonstrating that microtubules play a crucial role during the early stage of the ARV life cycle. In addition to regulating membrane docking and fusion in the early endocytic pathways, Rab5 sorting to the early endosome has also been proved to mediate both association of early endosomes with microtubules and early endosome motility toward the minus ends of microtubules (40). To further elucidate whether Rab5 is essential for ARV entry, we therefore used DN mutants of Rab5 to examine the requirement of transport to early endosomes in the entry of ARV. By investigating the molecular mechanisms that underlie ARV endocytosis, we have further observed that Rab5 has been implicated in ARV entry because depletion of Rab5 had a strong impact on ARV production, indicating that the participation of both microtubules and Rab5 for the early endosomes of ARV entry is required. Taken together, our results provide evidence suggesting that ARV cell entry via the caveolin1-mediated and dynamin-2-dependent endocytic pathway requires delivery to early endosome.

The ability of ARV to infect cells was greatly restricted using a specific inhibitor (bafilomycin A1) of the vacuolar proton-ATPase activity as well as lysomotropic agents, such as NH_4Cl and chloroquine. Notably, bafilomycin A1 may interfere with the endocytic route in two different ways. Bafilomycin A1 is known to prevent endosomal acidification by blocking vacuolar proton ATPase, but it also blocks the transport from early to late endosomes (37, 66). Direct support for the relevance of endocytic uptake for cell entry was provided by the inhibition of ARV infection with MβCD and nystatin together with

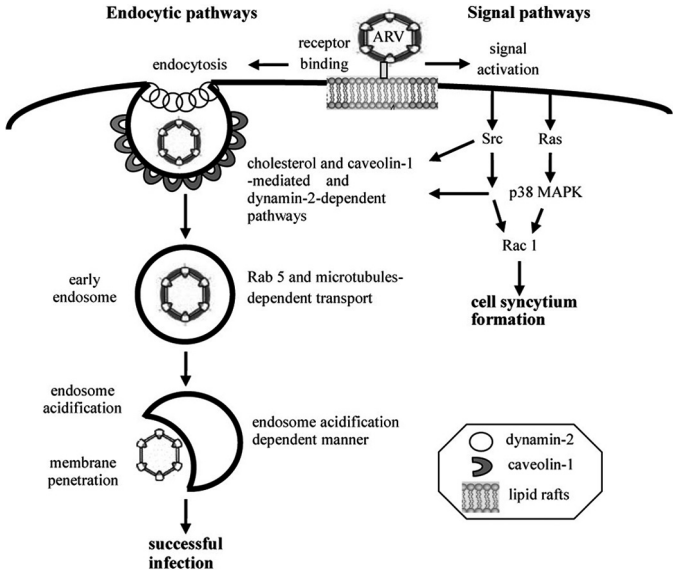

FIGURE 9. **Model of ARV entry and signal pathways involved in this process.** The incoming virion initially attached to the cell receptor is mediated by the outer capsid protein σC (25, 26) followed by receptor-mediated endocytosis. This study establishes the endocytic pathway used by ARV and the roles of various signaling molecules during ARV entry by examining the effects of selective inhibitors, DN mutants together with siRNAs targeting the caveolin-1 and dynamin-2. *Left side* depicts the major route of ARV entry, and the *right side* shows the signal pathways triggered by ARV. ARV induces Ras, p38 MAPK, Src, and Rac1 signaling during the early stage of the virus life cycle. Both p38 MAPK and Src were associated with caveolin-1 and dynamin-2 as demonstrated by reciprocal coimmunoprecipitation assays. p38 MAPK and Src signaling pathways triggered by ARV are involved in mediating phosphorylation of caveolin-1 and dynamin-2 expression. p38 MAPK and Src are upstream inducers of Rac1 facilitating cell syncytium formation.

dynamin-2 and caveolin-1 siRNA. ARV infection was strongly inhibited by inhibitors of endosomal acidification, indicating that ARV enters host cells by caveolin-1-mediated and dynamin-2-dependent endocytosis in a pH-dependent manner. Our findings suggest that the pH dependence of ARV entry and acidification of virus-containing endosomes are required for the ARV to uncoat and replicate within the host cells (67).

In summary, we have demonstrated that ARV has evolved to manipulate multiple signal pathways to enhance its entry and the formation of endocytic vesicles and subsequent trafficking. The signal pathways triggered by ARV play an important role in regulating both caveolin-1 and dynamin-2 expression, thereby increasing the rate of vesicle formation and subsequent trafficking. Furthermore, we have also provided evidence that ARV traffics to early endosomes in a process that requires the participation of microtubules and small GTPase Rab5. Taken together, our data strongly suggest that caveolin-mediated and dynamin-2-dependent endocytosis is a major route of ARV entry. After endocytosis, ARV requires transport to early endosomes before an acidic pH-dependent step presumably leads to the release of viral genome into the cytoplasm, resulting in productive infection. A schematic diagram depicting the signaling pathways and endocytic pathways required for ARV entry is shown in Fig. 9. The molecular mechanism identified in this study broadens our understanding of the pathways required for productive ARV and facilitates new strategies for combating ARV-caused diseases.

REFERENCES

1. Keen, J. H. (1990) *Annu. Rev. Biochem.* **59,** 415–438
2. Kirchhausen, T. (1999) *Annu. Rev. Cell Dev. Biol.* **15,** 705–732
3. Helenius, A., Kartenbeck, J., Simons, K., and Fries, E. (1980) *J. Cell Biol.* **84,** 404–420
4. Sieczkarski, S. B., and Whittaker, G. R. (2005) *Arch. Virol.* **150,** 1783–1796
5. Sun, X., Yau, V. K., Briggs, B. J., and Whittaker, G. R. (2005) *Virology* **338,** 53–60
6. Hommelgaard, A. M., Roepstorff, K., Vilhardt, F., Torgersen, M. L., Sandvig, K., and van Deurs, B. (2005) *Traffic* **6,** 720–724
7. Williams, T. M., and Lisanti, M. P. (2004) *Ann. Med.* **36,** 584–595
8. Jacobson, K., and Dietrich, C. (1999) *Trends Cell Biol.* **9,** 87–91
9. Westermann, M., Steiniger, F., Richter, W. (2005) *Histochem. Cell Biol.* **123,** 613–620
10. Hambleton, S., Steinberg, S. P., Gershon, M. D., and Gershon, A. A. (2007) *J. Virol.* **81,** 7548–7558
11. Henley, J. R., Krueger, E. W., Oswald, B. J., and McNiven, M. A. (1998) *J. Cell Biol.* **141,** 85–99
12. Hinshaw, J. E. (2000) *Annu. Rev. Cell Dev. Biol.* **16,** 483–519
13. Beer, C., Andersen, D. S., Rojek, A., and Pedersen, L. (2005) *J. Virol.* **79,** 10776–10787
14. Bousarghin, L., Touzé, A., Sizaret, P. Y., and Coursaget, P. (2003) *J. Virol.* **77,** 3846–3850
15. Empig, C. J., and Goldsmith, M. A. (2002) *J. Virol.* **76,** 5266–5270
16. Marjomäki, V., Pietiäinen, V., Matilainen, H., Upla, P., Ivaska, J., Nissinen, L., Reunanen, H., Huttunen, P., Hyypiä, T., and Heino, J. (2002) *J. Virol.* **76,** 1856–1865
17. Pietiäinen, V. M., Marjomäki, V., Heino, J., and Hyypiä, T. (2005) *Ann. Med.* **37,** 394–403
18. Damm, E. M., Pelkmans, L., Kartenbeck, J., Mezzacasa, A., Kurzchalia, T., and Helenius, A. (2005) *J. Cell Biol.* **168,** 477–488
19. Barnard, R. J., and Young, J. A. (2003) *Curr. Top. Microbiol. Immunol.* **281,** 107–136
20. Brindley, M. A., and Maury, W. (2005) *J. Virol.* **79,** 14482–14488
21. Skehel, J. J., and Wiley, D. C. (2000) *Annu. Rev. Biochem.* **69,** 531–569
22. Liu, H. J., Lin, P. Y., Wang, L. R., Hsu, H. Y., Liao, M. H., and Shih, W. L. (2008) *Mol. Cells* **26,** 396–403
23. Salsman, J., Top, D., Boutilier, J., and Duncan, R. (2005) *J. Virol.* **79,** 8090–8100
24. Chulu, J. L., Huang, W. R., Wang, L., Shih, W. L., and Liu, H. J. (2010) *J. Virol.* **84,** 7683–7694
25. Grande, A., Rodriguez, E., Costas, C., Everitt, E., and Benavente, J. (2000) *Virology* **274,** 367–377
26. Grande, A., Costas, C., and Benavente, J. (2002) *J. Gen. Virol.* **83,** 131–139
27. Shih, W. L., Hsu, H. W., Liao, M. H., Lee, L. H., and Liu, H. J. (2004) *Virology* **321,** 65–74
28. Liu, H. J., Lee, L. H., Hsu, H. W., Kuo, L. C., and Liao, M. H. (2003) *Virology* **314,** 336–349
29. Liu, H. J., Lin, P. Y., Lee, J. W., Hsu, H. Y., and Shih, W. L. (2005) *Biochem. Biophys. Res. Commun.* **336,** 709–715
30. Chulu, J. L., Lee, L. H., Lee, Y. C., Liao, S. H., Lin, F. L., Shih, W. L., and Liu, H. J. (2007) *Biochem. Biophys. Res. Commun.* **356,** 529–535
31. Ji, W. T., Lee, L. H., Lin, F. L., Wang, L., and Liu, H. J. (2009) *J. Gen. Virol.* **90,** 3002–3009
32. Lin, H. Y., Chuang, S. T., Chen, Y. T., Shih, W. L., Chang, C. D., and Liu, H. J. (2007) *Avian Pathol.* **36,** 155–159
33. Lin, P. Y., Lee, J. W., Liao, M. H., Hsu, H. Y., Chiu, S. J., Liu, H. J., and Shih, W. L. (2009) *Virology* **385,** 323–334
34. Hsu, C. J., Wang, C. Y., Lee, L. H., Shih, W. L., Chang, C. I., Cheng, H. L., Chulu, J. L., Ji, W. T., and Liu, H. J. (2006) *Avian Pathol.* **35,** 320–326
35. Sieczkarski, S. B., and Whittaker, G. R. (2003) *Traffic* **4,** 333–343
36. Macia, E., Ehrlich, M., Massol, R., Boucrot, E., Brunner, C., and Kirchhausen, T. (2006) *Dev. Cell* **10,** 839–850
37. Dröse, S., and Altendorf, K. (1997) *J. Exp. Biol.* **200,** 1–8
38. Vasquez, R. J., Howell, B., Yvon, A. M., Wadsworth, P., and Cassimeris, L. (1997) *Mol. Biol. Cell* **8,** 973–985
39. Heuser, J. E., and Anderson, R. G. (1989) *J. Cell Biol.* **108,** 389–400
40. Nielsen, E., Severin, F., Backer, J. M., Hyman, A. A., and Zerial, M. (1999) *Nat. Cell Biol.* **1,** 376–382
41. Roohvand, F., Maillard, P., Lavergne, J. P., Boulant, S., Walic, M., Andréo, U., Goueslain, L., Helle, F., Mallet, A., McLauchlan, J., and Budkowska, A. (2009) *J. Biol. Chem.* **284,** 13778–13791
42. Jordens, I., Marsman, M., Kuijl, C., and Neefjes, J. (2005) *Traffic* **6,** 1070–1077
43. Schimmöller, F., Simon, I., and Pfeffer, S. R. (1998) *J. Biol. Chem.* **273,** 22161–22164
44. Meertens, L., Bertaux, C., and Dragic, T. (2006) *J. Virol.* **80,** 11571–11578
45. Chazal, N., and Gerlier, D. (2003) *Microbiol. Mol. Biol. Rev.* **67,** 226–237
46. Mañes, S., del Real, G., and Martínez-A, C. (2003) *Nat. Rev. Immunol.* **3,** 557–568
47. Briggs, J. A., Wilk, T., and Fuller, S. D. (2003) *J. Gen. Virol.* **84,** 757–768
48. Aizaki, H., Lee, K. J., Sung, V. M., Ishiko, H., and Lai, M. M. (2004) *Virology* **324,** 450–461
49. Lee, C. J., Lin, H. R., Liao, C. L., and Lin, Y. L. (2008) *J. Virol.* **82,** 6470–6480
50. Parton, R. G., Hanzal-Bayer, M., Hancock, J. F. (2006) *J. Cell Sci.* **119,** 787–796
51. Shapiro, L., Heidenreich, K. A., Meintzer, M. K., and Dinarello, C. A. (1998) *Proc. Natl. Acad. Sci. U.S.A.* **95,** 7422–7426
52. Nakatsue, T., Katoh, I., Nakamura, S., Takahashi, Y., Ikawa, Y., and Yoshinaka, Y. (1998) *Biochim. Biophys. Res. Commun.* **253,** 59–64
53. McLean, T. I., and Bachenheimer, S. L. (1999) *J. Virol.* **73,** 8415–8426
54. Banerjee, S., Narayanan, K., Mizutani, T., and Makino, S. (2002) *J. Virol.* **76,** 5937–5948
55. Rahaus, M., Desloges, N., and Wolff, M. H. (2004) *J. Gen. Virol.* **85,** 3529–3540
56. Patel, H. H., Murray, F., and Insel, P. A. (2008) *Annu. Rev. Pharmacol. Toxicol.* **48,** 359–391
57. Pelkmans, L., Fava, E., Grabner, H., Hannus, M., Habermann, B., Krausz, E., and Zerial, M. (2005) *Nature* **436,** 78–86
58. Hall, A. (1998) *Science* **279,** 509–514
59. Giancotti, F. G., and Ruoslahti, E. (1999) *Science* **285,** 1028–1032
60. Yamada, K. M., and Even-Ram, S. (2002) *Nat. Cell Biol.* **4,** E75–E76
61. Etienne-Manneville, S., and Hall, A. (2002) *Nature* **420,** 629–635
62. Sahai, E., and Marshall, C. J. (2002) *Nat. Rev. Cancer* **2,** 133–142
63. Candurra, N. A., Lago, M. J., Maskin, L., and Damonte, E. B. (1999) *J. Gen. Virol.* **80,** 147–156
64. Campbell, E. M., Nunez, R., and Hope, T. J. (2004) *J. Virol.* **78,** 5745–5755
65. Ruthel, G., Demmin, G. L., Kallstrom, G., Javid, M. P., Badie, S. S., Will, A. B., Nelle, T., Schokman, R., Nguyen, T. L., Carra, J. H., Bavari, S., and Aman, M. J. (2005) *J. Virol.* **79,** 4709–4719
66. Bayer, N., Schober, D., Hüttinger, M., Blaas, D., and Fuchs, R. (2001) *J. Biol. Chem.* **276,** 3952–3962
67. Duncan, R. (1996) *Virology* **219,** 179–189